

## Pulse Field Gradient NMR Study of Diffusion of Pentane in Amorphous Glassy Perfluorodioxole

Ghirmai Meresi, Yingzi Wang, Job Cardoza, Wen Yang Wen, Alan A. Jones,\*  
Jaimie Gosselin, David Azar, and Paul T. Inglefield

Carlson School of Chemistry, Clark University, Worcester, Massachusetts 01610

Received January 18, 2001

**ABSTRACT:** Pulse field gradient diffusion measurements of pentane in a random copolymer of tetrafluoroethylene (TFE) and 2,2-bis(trifluoromethyl)-4,5-difluoro-1,3-dioxole (PDD) were made as a function of the time allowed for diffusion to occur. The initial change in echo amplitude at low values of  $q = \gamma \delta g$  was used to determine the apparent diffusion constant. The apparent diffusion constant determined in this way decreases to a constant value as time increases. At a time of 12.4 ms the apparent diffusion constant was  $2.2 \times 10^{-7} \text{ cm}^2 \text{ s}^{-1}$ , and it decreases to  $5.87 \times 10^{-8} \text{ cm}^2 \text{ s}^{-1}$  at 1 s. This change in the apparent diffusion constant was interpreted in terms of morphological structure on the micron length scale in this completely amorphous glassy polymer. This polymer has been considered to have high free volume regions which lead to the observed rapid permeation of gases and vapors. These regions are interspersed in lower free volume regions, and the low free volume regions constitute the majority component. In the pulse field gradient NMR experiment, regions allowing for rapid diffusion interspersed with regions allowing only slow diffusion can lead to changes in the apparent diffusion constant as a function of diffusion time. The data observed in this system were compared with two simple models for the topology of the regions allowing for rapid diffusion: restricted diffusion and tortuous diffusion. The observed behavior is qualitatively similar to tortuous diffusion and can be fit with an equation describing this type of diffusion.

### Introduction

The most permeable fluoropolymer known is the random copolymer of tetrafluoroethylene (TFE) and 2,2-bis(trifluoromethyl)-4,5-difluoro-1,3-dioxole (PDD).<sup>1–4</sup> This polymer exhibits high solubility and high translational diffusion of gases, small hydrocarbons, and small fluorocarbons. Solubility can be described by the dual-mode model, and the high solubility results mostly from the Henry's law contribution.<sup>5,6</sup> The copolymer is produced as a commercial product by Dupont with two compositions: 13 and 35 mol % tetrafluoroethylene. The glass transition temperatures are 240 and 160 °C, respectively.

The bulky dioxole rings in the backbone of this polymer lead to the high glass transition temperature, but interestingly it also leads to a high fractional free volume of 0.32, which indicates poor chain packing. This in turn contributes to the observed high permeability. The size of the free volume elements in this polymer have been characterized by positron annihilation lifetime spectroscopy (PALS).<sup>1,7</sup> The largest free volume elements have a size ranging from 0.59 to 0.64 nm<sup>3</sup> and are considered to be grouped in larger disordered regions. The fraction of free volume in these disordered regions is 0.03–0.04 when the fraction of PDD in the copolymer is 0.87. The corresponding fraction is 0.001–0.003 in conventional glassy polymers which also have smaller free volume elements (0.3–0.4 nm).

The PDD/TFE copolymer is similar in some ways to another polymer of this general type, poly(1-trimethylsilyl-1-propyne) (PTMSP), which also has bulky backbone units, a high glass transition temperature, and comparable fractional free volume. The free volume elements are slightly larger in PTMSP, 0.6–0.7 nm, but the fraction of free volume in the high free volume,

disordered regions is 0.10, which is significantly greater than PDD/TFE.

PTMSP has significantly higher permeability which has been attributed to the higher fraction of free volume in the disordered regions. It has been suggested that the high free volume regions in PTMSP might be interconnected, providing a pathway for rapid permeation while the high free volume regions in PDD/TFE are more isolated or more poorly connected.<sup>4</sup>

Currently, there is little direct evidence on the size of the high free volume regions or the interconnectedness in this type of polymer. The high free volume elements located in these regions are 0.6 nm according to PALS, but if they are grouped together in domains, then the question of the size of these domains remains to be determined. Pulse field gradient (PFG) NMR can address the size and the interconnectedness of regions which allow for rapid translational diffusion when these regions are surrounded by regions which are impenetrable or much less penetrable.<sup>8,10–12</sup>

If a region that accommodates rapid diffusion is surrounded by an impenetrable barrier, there are well-established descriptions of what will be observed in a PFG NMR experiment.<sup>8</sup> This situation is referred to as restricted diffusion. For typical gradient strengths and diffusion constants, the length scale of the restricted domain which can be probed is tenths to tens of microns. In systems where the regions that accommodate rapid diffusion are interconnected but still impeded by regions that do not support rapid diffusion, the process of long-range diffusion is described as tortuous.<sup>9–12</sup> Again, a quantitative model for the behavior in a PFG NMR experiment is available, and the length scale characterizing the two types of regions which can typically be detected falls in the micron range.

Systems with tortuous diffusion are often porous where the pores are essentially free space, and diffusion of gases or liquids within these spaces is described by the diffusion constant of the pure gas or liquid. Examples of porous systems include activated charcoal,<sup>13,14</sup> zeolites,<sup>15</sup> and limestone.<sup>11</sup> Restricted diffusion has been observed in bounded systems such as cells and micelles.<sup>16</sup> While we are not aware of any polymer systems that display restricted diffusion, semicrystalline polymers display tortuous diffusion.<sup>8</sup> In this case the crystals are the impenetrable barriers to diffusion, and the amorphous phase provides the more rapid translational diffusion path. Classical tortuous PFG NMR data were obtained by Veeman et al.<sup>12</sup> in a semicrystalline polymer where the penetrant was xenon gas. In this case the apparent diffusion constant is a strong function of the time during which diffusion is allowed to occur in the PFG NMR experiment. The apparent diffusion constant decreases to a plateau value as the time increases.

A quantitative model is available for the interpretation of such data,<sup>9–11</sup> but in the case of a semicrystalline polymer the diffusion constant in the amorphous phase would not be the diffusion constant of the pure penetrant. To a first approximation this would be replaced by the diffusion constant in a completely amorphous sample of the polymer, and then the effect of the crystalline domains in the semicrystalline sample could be treated with the model for tortuosity.

High-permeability polymers like PTMSP or PDD/TFE might be considered as “porous” systems or restricted systems depending on the level of interconnectedness of the disordered high free volume regions. However, the disordered regions that contain subnanometer sized free volume elements and support rapid transport may not approximate empty space, and diffusion within this region may not be described by the diffusion constant of the pure penetrant. Quite possibly the diffusion constant in the disordered region would be lower than that of the pure penetrant, but then maybe the picture of porosity and tortuosity would apply in the same way as it does to semicrystalline polymers. On the other hand, tortuosity has been used to describe activated charcoals with subnanometer-sized pores and pure solvent diffusion constants.<sup>13,14</sup>

To test the applicability of these models to the copolymer PDD/TFE, the observed apparent diffusion constant of pentane measured as a function of the time allowed for diffusion<sup>17</sup> will be compared qualitatively with the predictions of simple models for restricted diffusion and tortuosity. If the behavior is close to one of the simple model predictions, then the appropriate model can be quantitatively applied. For restricted diffusion this could lead to length scale information, and for tortuous diffusion this could test how close the disordered regions come to being interconnected pores.

## Experimental Section

An 8 wt % pentane was prepared by adding the appropriate amount of penetrant to a cast film of PDD/TFE and was then sealed in a 5 mm NMR tube. The film was cast from a perfluoroheptane solution and was dried to constant weight in a vacuum oven at 50 °C. The copolymer was AF1600 (Dupont Trademark) and was provided by Dupont. The penetrant/film system equilibrated for a period of days before measurements were made, and no changes in the mobility of the penetrant were observed over a period of weeks during

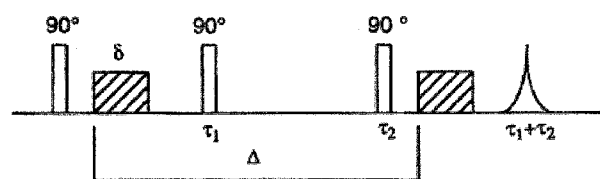


**Figure 1.** Stimulated echo pulse gradient sequence used to determine  $D$  as a function of diffusion time ( $\Delta$ ).

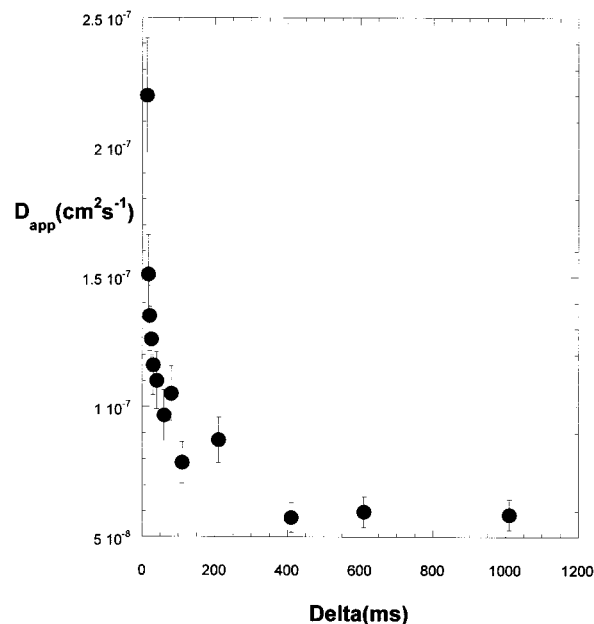


**Figure 2.**  $D_{app}$  vs  $\Delta$  for 8 wt % pentane in AF 1600 at 26 °C.

which measurements were made. Glass spacers were used in the NMR tube to center the sample of the correct size in the region of the radio-frequency and gradient coils. The apparent diffusion constant of the penetrant,  $D$ , was measured as a function of the diffusion time,  $\Delta$ , indicated in the stimulated echo pulse sequence shown in Figure 1. The diffusion time,  $\Delta$ , ranged from 10 ms to 1 s at low values of the quantity  $q = \gamma \delta g / 2\pi$ . A fixed value of  $\delta$  of 8 ms was used for a given determination of the apparent diffusion constant. The gradient strength was varied to obtain the apparent diffusion constant from a plot of the logarithm of the echo amplitude vs  $g^2$ . The maximum value of  $g$  in each determination ranged from 20 to 100 G/cm. In all cases, the echo amplitude decrease at the maximum  $g$  value was less than 50% of the initial amplitude. The measurements were made at 26 °C on a Varian Inova 400 MHz wide-bore NMR spectrometer with a  $^1\text{H}$ ( $^{15}\text{N}$ – $^{31}\text{P}$ ) 5 mm PFG indirect detection probe by observing proton signals from the penetrant.

Proton spin–lattice relaxation times were also measured on the pentane in the PDD/TFE film using a  $180$ – $\tau$ – $90$  pulse sequence on Varian Mercury 200.

## Results

The plots of the logarithm of echo amplitude vs  $g^2$  were linear, yielding a value of  $D$  for each diffusion time  $\Delta$ . Figure 2 contains a plot of  $D$  as a function of the time  $\Delta$ . The proton spin–lattice relaxation time at 26 °C is 2.5 s at a Larmor frequency of 200 MHz.

**Interpretation.** Two straightforward models can be used to predict the behavior of the apparent diffusion constant  $D$  on  $\Delta$ . The models are likely oversimplifications of the actual situation likely to be encountered in polymers but can at least serve to identify different behavior. The first model is restricted diffusion in one

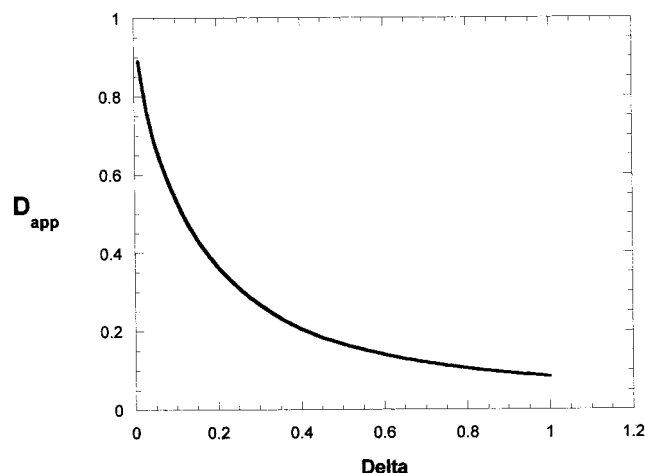


**Figure 3.** Apparent calculated diffusion constant vs the time for diffusion in the PFG experiment for the restricted diffusion model. The barrier spacing ( $a$ ) equals 1, the diffusion constant between barriers equals 100, and in the limit of large  $\Delta$  the product of the apparent diffusion constant times  $\Delta$  equals  $1/12a^2$  or 0.084.

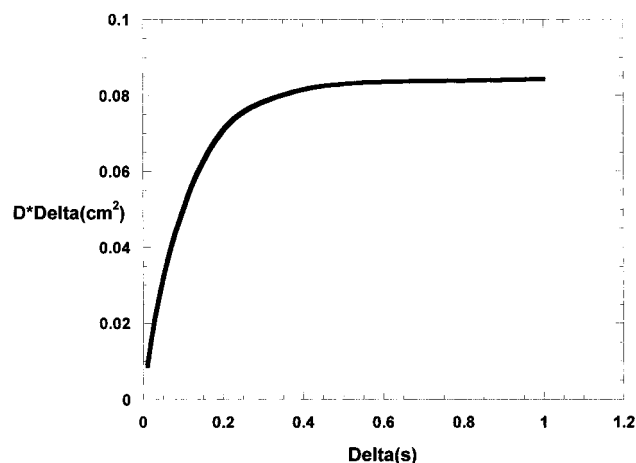


**Figure 4.**  $D_{app}\Delta$  vs  $\Delta$  for the restricted diffusion model described in Figure 3.

dimension. The equation for echo amplitude  $E(q)$  is

$$E(q) = \frac{2\{1 - \cos(2\pi qa)\}}{(2\pi qa)^2} + 4(\pi qa)^2 \sum_{n=1}^{\infty} \exp\left(-\frac{n^2 \pi^2 D \Delta}{a^2}\right) \frac{1 - (-1)^n \cos(2\pi qa)}{\{(2\pi qa)^2 - (n\pi)^2\}^2} \quad (1)$$

where  $a$  is the spacing between barriers and  $D$  is the diffusion constant between barriers. To utilize this equation, an apparent  $D$  ( $D_{app}$ ) is calculated from the initial decay of  $E$  vs  $q^2$  for a specific choice of  $a$  and the diffusion constant between barriers plus a given choice of  $\Delta$ . To obtain the trend of the apparent diffusion constant as a function of  $\Delta$ , the calculation is repeated for different  $\Delta$ 's. The result for an arbitrary choice of spacing and diffusion constant between barriers for the apparent diffusion constant as a function of  $\Delta$  is shown in Figure 3. The characteristic result for restricted diffusion is that the apparent  $D_{app}$  continually decreases as  $\Delta$  increases. The value of the product  $D_{app}\Delta$  shown in Figure 4 becomes constant at large  $\Delta$  and equals  $a^2/12$ . The experimental data of Figure 2 do not continually decrease at large  $\Delta$  as the model does in Figure 3 but

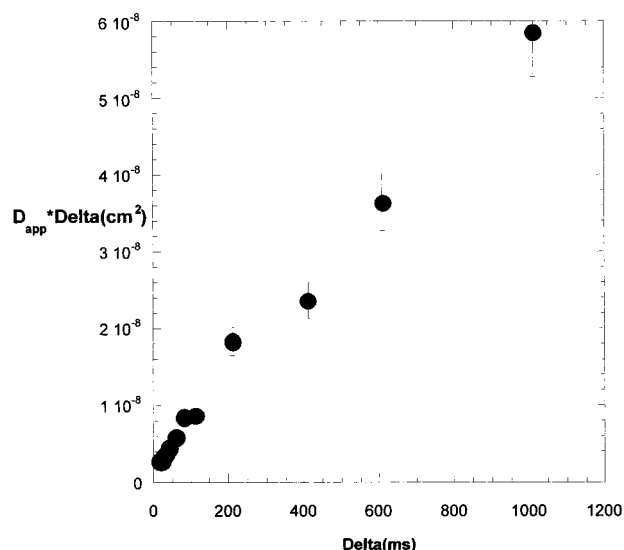


**Figure 5.**  $D_{app}\Delta$  vs  $\Delta$  for 8 wt % pentane in AF 1600 at 26 °C.

rather reach a plateau value. If the product of the experimental apparent diffusion constant and the time  $\Delta$  is calculated and plotted as shown in Figure 5, it does not become constant but rather monotonically increases.

The second simple model is for a porous system where diffusion is tortuous. This is a model developed to characterize diffusion of water in porous rock and was based on diffusion through random packed impenetrable spheres. Here an equation for the apparent diffusion constant at a given value of  $\Delta$  divided by the diffusion constant for the pure penetrant,  $D_0$ , is

$$\frac{D_{app}(\Delta)}{D_0} = 1 - \left(1 - \frac{1}{\alpha}\right) \left\{ \frac{c\sqrt{\Delta} + \left(1 - \frac{1}{\alpha}\right)\frac{\Delta}{\theta}}{\left(1 - \frac{1}{\alpha}\right) + c\sqrt{\Delta} + \left(1 - \frac{1}{\alpha}\right)\frac{\Delta}{\theta}} \right\} \quad (2)$$

The tortuosity is represented by  $\alpha$  and  $c$  is given by the equation

$$c = \frac{4}{9\sqrt{\pi}} \left(\frac{S}{V}\right) \sqrt{D_0} \quad (3)$$

where  $S/V$  = the surface-to-volume ratio and  $\theta$  is given by

$$\theta = 0.147 \frac{d^2}{D_0} \quad (4)$$

For spherical bead packs,  $d$  is the diameter of the spheres. The surface-to-volume ratio is also related to  $d$  by

$$\frac{S}{V} = \frac{6\left(\frac{1}{\phi} - 1\right)}{d} \quad (5)$$

where  $\phi$  is the porosity. A prediction of the dependence of  $D_{app}$  on  $\Delta$  for this model for tortuous diffusion based on eq 2 is given in Figure 6. This model predicts that the  $D_{app}$  becomes constant at large  $\Delta$ , and thus the product  $D_{app}\Delta$  linearly increases with  $\Delta$  at large  $\Delta$ . These predictions are qualitatively similar to the ex-

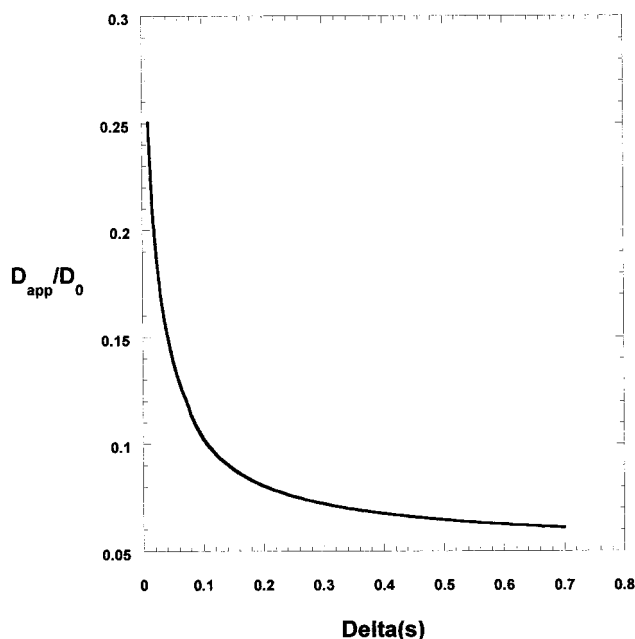


**Figure 6.** Apparent calculated diffusion constant divided by the diffusion constant for pure penetrant vs time in the PFG experiment for the tortuosity model. The model parameters are  $D_0 = 3.1 \times 10^{-7} \text{ cm}^2 \text{ s}^{-1}$ ,  $\alpha = 20$ ,  $\theta = 0.01$ ,  $\varphi = 0.03$ , and  $d = 10 \text{ }\mu\text{m}$ .

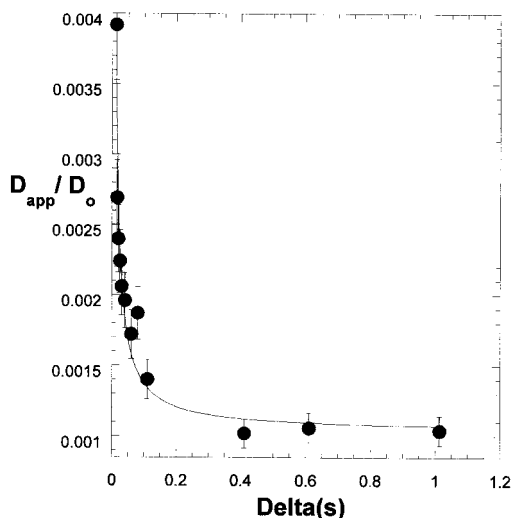


**Figure 7.**  $D_{\text{app}}/D_0$  vs  $\Delta$  for 8 wt % pentane in AF 1600 at 26 °C fit to the tortuosity model as described in the text.

perimental data for pentane in PDD/TFE given in Figures 2 and 5.

A nonlinear least-squares fit of eq 2 to the data in Figure 2 can be attempted. At short times  $\Delta$ , the quantity  $D_{\text{app}}/D_0$  should be linear with the square root of  $\Delta$ , but the data in hand do not follow this dependence. Thus, no estimate of  $D_0$  is possible from the data although  $D_0$  could be assumed to be equal to that for pure pentane. If this value of  $D_0$  is assumed ( $D_0 = 5.62 \times 10^{-5} \text{ cm}^2 \text{ s}^{-1}$  at 25 °C), the tortuosity,  $\alpha$ , can be calculated from the long time behavior in Figure 2 since  $D_{\text{app}}$  becomes independent of  $\Delta$ . This leads to a value of  $\alpha = 9.6 \times 10^2$  using the value of  $D_{\text{app}} = 5.87 \times 10^{-8} \text{ cm}^2 \text{ s}^{-1}$  at  $\Delta = 1 \text{ s}$ . Figure 7 shows a fit of the data plotted as  $D_{\text{app}}/D_0$  vs  $\Delta$  fixing the values of  $D_0$  and  $\alpha$  as just discussed and varying the quantities  $c$  and  $\theta$ . The fit is within the experimental error of the data, but the value of  $c$  is not well determined since it is controlled by the

short time data. As already discussed, the short time data do not extend to small enough values. The value of  $\theta$  is better determined but is dependent on the choice of  $D_0$  and  $\alpha$ . Equally good fits are obtained for  $D_0$ 's ranging down to  $2 \times 10^{-6} \text{ cm}^2 \text{ s}^{-1}$ .

## Discussion

The dependence of the apparent diffusion constant on the diffusion time  $\Delta$  qualitatively appears like tortuous diffusion in a porous medium. The data can be fit assuming the value of  $D_0$  for pure pentane which leads to a value of the tortuosity near 1000. It is not a unique fit and depends on the initial choice of  $D_0$ . This is a very high value of tortuosity but similar to values observed for activated charcoals with subnanometer sized pores and a porosity of a couple of hundredths.<sup>13,14</sup> The activated charcoals have no structure in the micron range, and so they display no dependence of  $D_{\text{app}}$  on  $\Delta$  under experimental conditions similar to those used here.<sup>13,14</sup>

Should one really consider PDD/TFE to be a porous system? This would be an extreme view even given the results presented so far. The value of  $D_0$  used in the analysis was arbitrarily set to that of pure pentane, and smaller values of  $D_0$  provide equally good fits. If the system can be considered in the framework of eq 2, some smaller value of  $D_0$  would be likely for pentane even in a high free volume region of the copolymer. This value might be identified if the data could be extended to shorter times through the use of significantly higher gradients (work which is currently underway).

The presence of structure influencing diffusion on the micron length scale is likely since there is a significant dependence of the apparent diffusion constant on  $\Delta$ . This conclusion is indicated by the data whether or not the term "porous" should be applied. Diffusion has been measured in other polymer systems with comparable diffusion constants, and no dependence of  $D$  on  $\Delta$  was observed. The possibility of local internal field gradients produced by the sample was considered, but more sophisticated pulse sequences<sup>10</sup> produced the same apparent diffusion constants. Cross-relaxation between the polymer and the penetrant is not possible since the polymer is fluorinated and the penetrant is protonated.<sup>18</sup>  $D_{\text{app}}$  might consist of two components with different  $D$ 's and different  $T_1$ 's. However, the echo decays are linear, and the amplitudes of the signals in the inversion–recovery experiment are well described by a single  $T_1$ . If there are two  $D$ 's and two  $T_1$ 's, they do not differ greatly. Thus, the change in  $D_{\text{app}}$  with  $\Delta$  is ascribed to the presence of morphological structure. Since the dependence is similar to tortuous diffusion in a porous medium, the view that there is fast diffusion in high free volume regions surrounded by regions with slow diffusion seems plausible. This view was suggested<sup>1,4</sup> earlier for this type of high permeability polymers prior to the PFG NMR experiments, and the results obtained here now lend more credibility to this possibility.

The development of PFG NMR data on other small molecules and on other high-permeability polymers should help in developing a better understanding of these systems. As mentioned, extending data to shorter diffusion times using higher gradients may also help to clarify these systems.

**Acknowledgment.** This research was carried out with the financial support of the National Science Foundation Grant DMR-9901416.



## References and Notes

- (1) Alentiev, A. Y.; Yamploski, Y. P.; Shantarovich, V. P.; Nemser, S. M.; Plate, N. A. *J. Membr. Sci.* **1997**, *126*, 123.
- (2) Merkel, T. C.; Bondar, V.; Nagai, K.; Freeman, B. D. *Macromolecules* **1999**, *32*, 370.
- (3) Bondar, V. I.; Freeman, B. D.; Yampolskii, Yu. P. *Macromolecules* **1999**, *32*, 6163.
- (4) Singh, A.; Bondar, S.; Dixon, S.; Freeman, B. D.; Hill, A. J. *Proc. Am. Chem. Soc. Div. Polym. Mater.: Sci. Eng.* **1997**, *77*, 316.
- (5) Bondar, V. I.; Freeman, B. D.; Yampolskii, Yu. P. *Macromolecules* **1999**, *32*, 6163.
- (6) Merkel, T. C.; Bondar, V.; Nagai, K.; Freeman, B. D. *Macromolecules* **1999**, *32*, 370.
- (7) Yampolskii, Yu. P.; Shantarovich, V. P. In *Polymer Membranes for Gas and Vapor Separation*; ACS Symposium Series No. 733; Freeman, B. D., Pinnau, I., Eds.; American Chemical Society: Washington, DC, 1999; pp 102–114.
- (8) Callaghan, P. T. *Principles of Nuclear Magnetic Resonance Microscopy*; Oxford University Press: New York, 1991.
- (9) Mitra, P. P.; Sen, P. N.; Schwartz, L. M.; Le Doussal, P. *Phys. Rev. Lett.* **1992**, *68*, 3555.
- (10) Latour, L. L.; Mitra, P. P.; Kleinberg, R. L.; Sotak, C. H. *J. Magn. Reson. A* **1993**, *101*, 342.
- (11) Latour, L. L.; Kleinberg, R. L.; Mitra, P. P.; Sotak, C. H. *J. Magn. Reson. A* **1995**, *112*, 83.
- (12) Veeman, W. S.; Junker, F. *Proc. Am. Chem. Soc. Div. Polym. Mater.: Sci. Eng.* **2000**, *82*, 167.
- (13) Dubinin, M. M.; Yartapetian, R. S.; Voloshchuk, A. M.; Karger, J.; Pfeifer, H. *Carbon* **1988**, *26*, 515.
- (14) Schieferstein, E.; Heinrich, P. *Langmuir* **1997**, *13*, 1723.
- (15) Karger, J.; Pfeifer, H. *Zeolites* **1987**, *7*, 90.
- (16) Tanner, J. E.; Stejskal, E. O. *J. Chem. Phys.* **1968**, *49*, 1768.
- (17) Meresi, G.; Wang, Y.; Cardoza, J.; Wen, W.-Y.; Jones, A. A.; Inglefield, P. T. *Macromolecules* **2001**, *34*, 1131.
- (18) Peschier, L. J. C.; Bouwstra, J. A.; de Bleyser, J.; Junginger, H. E.; Leyte, J. C. *J. Magn. Reson. B* **1996**, *110*, 159.

MA010094C